

See discussions, stats, and author profiles for this publication at: <https://www.researchgate.net/publication/269231960>

# Fabricate Wavy Micro/Nano Fiber via Auxiliary Electrodes

Conference Paper · January 2014

DOI: 10.3850/978-981-09-0446-3\_063

CITATIONS

2

READS

113

6 authors, including:



[Ziming Zhu](#)

GuangDong University of Technology

8 PUBLICATIONS 27 CITATIONS

[SEE PROFILE](#)



[Xindu Chen](#)

GuangDong University of Technology

47 PUBLICATIONS 192 CITATIONS

[SEE PROFILE](#)



[Feng Liang](#)

GuangDong University of Technology

9 PUBLICATIONS 14 CITATIONS

[SEE PROFILE](#)



[Han Wang](#)

GuangDong University of Technology

57 PUBLICATIONS 226 CITATIONS

[SEE PROFILE](#)

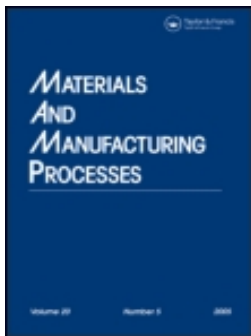
Some of the authors of this publication are also working on these related projects:



Approximation Strategies and Parallel Computing Methods for Large-scale Stochastic RCPSP & RCMPSP [View project](#)



HoJun Jeon [View project](#)



## Fabricated Wavy Micro/Nanofiber via Auxiliary Electrodes in Near-Field Electrospinning

Ziming Zhu, Xindu Chen, Zefeng Du, Shenneng Huang, Dongyu Peng, Junwei Zheng & Han Wang

**To cite this article:** Ziming Zhu, Xindu Chen, Zefeng Du, Shenneng Huang, Dongyu Peng, Junwei Zheng & Han Wang (2016) Fabricated Wavy Micro/Nanofiber via Auxiliary Electrodes in Near-Field Electrospinning, *Materials and Manufacturing Processes*, 31:6, 707-712, DOI: [10.1080/10426914.2015.1048464](https://doi.org/10.1080/10426914.2015.1048464)

**To link to this article:** <http://dx.doi.org/10.1080/10426914.2015.1048464>



Accepted author version posted online: 29 May 2015.  
Published online: 29 May 2015.



Submit your article to this journal [↗](#)



Article views: 177



View related articles [↗](#)



View Crossmark data [↗](#)

# Fabricated Wavy Micro/Nanofiber via Auxiliary Electrodes in Near-Field Electrospinning

ZIMING ZHU, XINDU CHEN, ZEFENG DU, SHENNENG HUANG, DONGYU PENG, JUNWEI ZHENG, AND HAN WANG

*Guangdong Provincial Key Laboratory of Micro-nano Manufacturing Technology and Equipment, Guangdong University of Technology, Guangzhou, Guangdong, China*

Wavy fibers fabricated by electrohydrodynamic jet printing (E-J-P) have been used in many applications, such as sensors, electromechanical systems, stretchable electronics products, and flexible displays. Auxiliary electrodes (A-E) were initially used to control the deposited morphology of the wavy fibers in this study. A polyethylene oxide solution was electrospun with an applied voltage of 1 kV and an alternating current power (ACP) supplied to A-E. The experimental results show that the amplitude can be controlled by the voltage of the ACP, and the generated frequency of the wavy fiber is the same as the frequency of the ACP.

**Keywords** Auxiliary electrode; Electrohydrodynamic jet printing; Electrospinning; Near-field electrospinning; Wavy fiber.

## INTRODUCTION

Electrospinning is a simple, economic, and versatile technique for fabricating ultrafine fibers with diameters ranging from 5 nm to 3  $\mu$ m. Materials, including polymers, metals, ceramics, etc., are best constructed by such small-scale fibers [1]. Since electrospinning was first introduced by Formhals in 1934, it has been widely studied by many people since the 1990s [2]. Wavy micro/nanofiber, caused by bending instability, is a common phenomenon in traditional electrospinning. Besides, when the collector speed is low, wavy fiber also appears in the near-field electrospinning (NFES). Due to their unique structure, the wavy micro/nanofibers, fabricated by the electrohydrodynamic jet printing (E-J-P), have been used in many applications, for instance, sensors and resonators, electromechanical systems, electromagnetic devices, stretchable electronics products, flexible displays, and electronic skin [3–8].

In 2000, Reneker first introduced bending instability in electrospinning. It was discovered that during the jet drop from the capillary to the collector, the jet would become unstable resulting in the definition of bending instability. During the electrospinning process, the jet coils when it impacts a hard, stationary surface followed by buckling. As a result, a helical, or wavy, fiber is found on the collector due to the small bending instability [9]. Yarin et al. established a mathematical model to describe the bending instability [10]. Zhao et al. demonstrated how

the solution concentration affects the morphologies of the fibers, and as the concentration increased, products appear with a variety of morphologies, including polymer colloids, beaded fibers, smooth fibers, and zigzag ribbons [11]. Han et al. learned that the buckling instability in electrospinning has patterns with frequencies of the order of  $10^5$ – $10^6$  Hz [12]. Meanwhile, the deposited buckling resulted in sinuous, zigzag-like, figures-of-eight, recurring curves, coiled, and other microstructures, which are similar to many patterns created by uncharged jets as the highly viscous fluids impinge hard flat surfaces. Han found a new phenomenon called pendulum-like jet that was caused by the repulsive Coulomb force between the straight electrified jet and the charges accumulated on the collector [13]. Additionally, The zigzag fibers were collected on a static water surface and had patterns with frequencies of the order of 10 to  $10^2$  Hz. NFES was first studied by Sun, who designated it as a new technique to fabricate straight fibers and alignment with a moving collector [14]. However, Zheng found that the wavy fibers could also be composed when the collector speed was slow during the NFES process [15]. Xin et al. built a moving collector with a gas-controlled lateral motion used to collect buckled fibers. The conditions for making these swinging patterns are reproducible, and at the same time, these uniform buckled patterns extend over millimeter distances [16]. Duan et al. introduced a new method to fabricate wavy fibers by implementing photolithography to generate well-defined patterns [17]. In order to get fibers with specific wavy/coiled microstructures, auxiliary electric field and patterned collectors have been used to control fibers deposition process [18, 19]. Sun et al. developed a novel electrospinning method for fabricating curled fibers, which required reciprocating-type electrospinning [20]. This method combined whipping-based electrospinning and detachment lithography to generate

Received August 7, 2014; Accepted April 12, 2015

Address correspondence to Han Wang, Room 108, Engineering Building #2, Guangdong University of Technology, Guangzhou Higher Education Mega Center, Guangzhou 510006, China; E-mail: wanghangood@gdut.edu.cn

Color versions of one or more of the figures in the article can be found online at [www.tandfonline.com/lmmp](http://www.tandfonline.com/lmmp).

patterned film with high stretchability. Duan et al. presented a new method to fabricate nonwrinkled and highly stretchable wavy fibers in which straight fibers were directly written on a prestrained substrate, followed by release of the substrate and the appearance of wavy fibers appear [21]. Gu used a rotated electric field to fabricate twisted nanofibers for use in artificial muscles [22].

Those methods mentioned above for fabricating wavy fibers are, unfortunately, too rough to be used in electronic devices. NFES can accurately deposit high-positioned fibers by shortening the nozzle-to-collector distance; however, the generated fibers are normally straight or uncontrollable [17, 23–29]. Although auxiliary electric field has been applied to control the morphology of the fibers in the conventional electrospinning process, the major purpose of using auxiliary electric field was to align fibers [18, 23, 30–33].

In this paper, NFES and auxiliary electric field are initially combined to fabricate a pattern-controllable wavy fiber. The NFES is utilized to accurately generate high-positioned fibers, and the auxiliary electric field is employed to control the morphology of the deposited fibers. Compared with traditional methods to generate wavy fibers, the fibrous morphology can be controlled by means of auxiliary electrodes (A-E), and the generated frequencies of wavy fibers would be controlled by the alternating current power (ACP) frequencies. This method is highly significant in fabricating zigzag fibers, which can be used to produce the codes of the grating. Normally, most of the grating codes on the grating ruler are created by laser carve, which is very difficult and expensive for gratings whose diameters are less than  $5\text{ }\mu\text{m}$  [34]. However, NFES can produce fibers with diameters ranging from  $50\text{ nm}$  to  $3\text{ }\mu\text{m}$ , which is significant for construction of the lines of the grating ruler [35].

#### MATERIALS AND METHODS

Poly (ethylene oxide) (PEO),  $M_w = 2000,000\text{ g}\cdot\text{mol}^{-1}$ , 3–6 wt% solution in distilled water and under stirring for 4 h at room temperature  $20^\circ\text{C}$ . PEO was purchased from Aladdin, Shanghai, China, and the distilled water was purchased from Watsons (Guangzhou, China). The ground collector was made of chromium plating glass, which is also the material for fabricating grating.

The experimental setup, shown in Fig. 1, for NFES is the same as those used previously, at constant room temperature of  $20^\circ\text{C}$  and relative humidity of about 50% [14, 15]. However, there are two parallel A-E setting on the collector, and the upper surface of the collector is higher than the lower edge of the parallel A-E. Meanwhile, the tip of the nozzle is lower than the upper edge of the parallel A-E, both of which can avoid the marginal effects of the electric field. The nozzle size is 30 G with an inner diameter of  $0.16\text{ mm}$  and outer diameter of  $0.31\text{ mm}$ . The collector can move at a constant speed of typically  $V_C = 0\text{--}45\text{ mm/s}$  via a motion platform (SURUGA, JAPAN). The syringe and the accurate syringe pump were installed on an X-Y-Z manual operation accurate platform, which can be adjusted to the distance

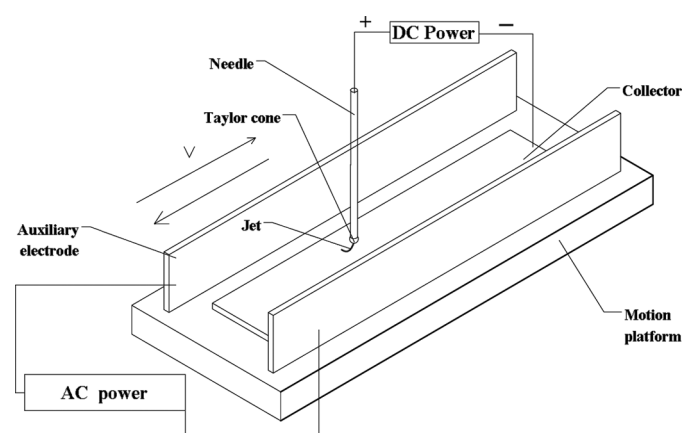


FIGURE 1.—Schematic representation of the experimental setup.

between the nozzle and collector with the help of the microcalliper. The range of the direct current (DC) power is  $0\text{--}50\text{ kV}$ , the range of ACP supplied to A-E is  $0\text{--}5\text{ kV}$ , and its frequency range is  $49\text{--}490\text{ kHz}$  (SUN, SNP-605). The wavy shape of ACP voltage is shown in Fig. 2. The A-E is made of copper foil, and the distance of two A-E is  $40\text{ mm}$ .

In this paper, ACP voltage and ACP voltage frequencies are studied, and the experimental parameters are selected from the most suitable parameters of previous works [36–38]. The PEO fibers were collected on the collector with the speed  $5\text{ mm/s}$ . The ACP voltages supplied to auxiliary selected were  $0, 1250, 2500, 3750$ , and  $5000\text{ V}$ . The nozzle to collector distance was  $4\text{ mm}$ , and the DC power supply voltage to the nozzle was  $1\text{ kV}$ . The frequency of the ACP voltage was  $50\text{ Hz}$ . On the other hand, the experimental parameters for “the ACP voltage frequencies parameter” were as follows: distance between nozzle and collector (D-N-C) was  $4\text{ mm}$ , the

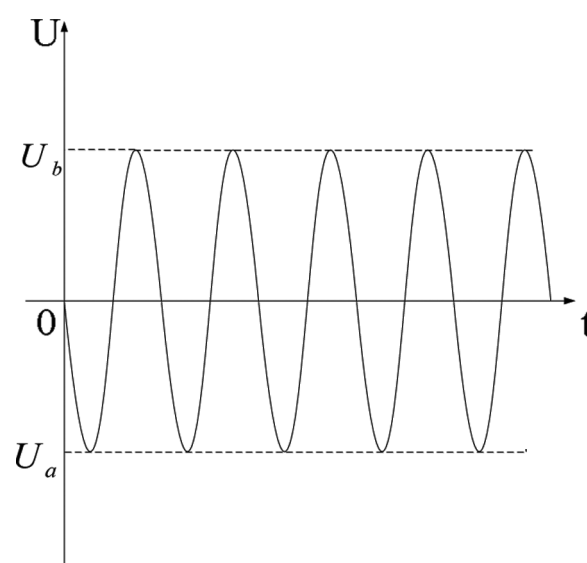


FIGURE 2.—Wave shape of ACP voltage.

solution concentration was 4 wt%, the applied voltage was 1 kV, the collector speed was 10 mm/s, and the ACP voltage was 2000 V. The selected frequencies of the ACP were 50, 100, 150, and 200 Hz.

The microstructure was characterized by computer numerical control (CNC) video measuring system (VMS-3020H, Rational, China). Scanning electron microscopy (SEM) (HITACHI TM3030, Hitachi, Japan) was used to characterize the electrospun nanofibers, and the SEM scanning voltage was 5 kV.

## RESULTS AND DISCUSSION

During the NFES process, the jet drops from the nozzle to the motion collector, then the nanofiber can be deposited along the track of collector. The jet stays straight and cannot be collected as a regular wavy/coils fiber unless supplies the ACP voltage to A-E, as shown in Fig. 3(a). When the ACP voltage is supplied to the A-E, there is an alternating electric field (50 Hz) between the two A-E terminals caused by the ACP voltage. When the “alternating electrical field” force plays a more important role in the NFES deposition process, the charged jet begins to swing. Therefore, the wavy fibers’ morphology is deposited on the collector with control. Meanwhile, the amplitude of the deposited fibers increases as the ACP voltage increases, which are shown in Fig. 3(b)–(e). The amplitude of the fiber has a linear relation with the collector speed (Fig. 4(a)), and the fibrous amplitude increases along with the ACP voltage increases (Fig. 4(b)). Thus, the amplitude of the

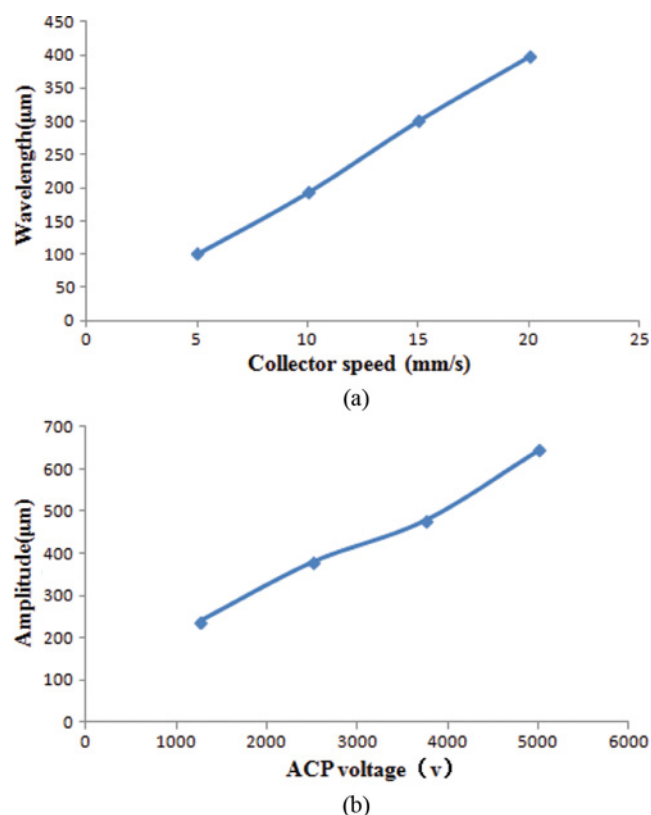


FIGURE 4.—Experimental parameter: the applied voltage to nozzle is 1 kV, the D-N-C is 4 mm, and the solution is 4 wt%. (a) Fiber wavelength versus collector speed; (b) wavy fiber amplitude versus ACP voltage.

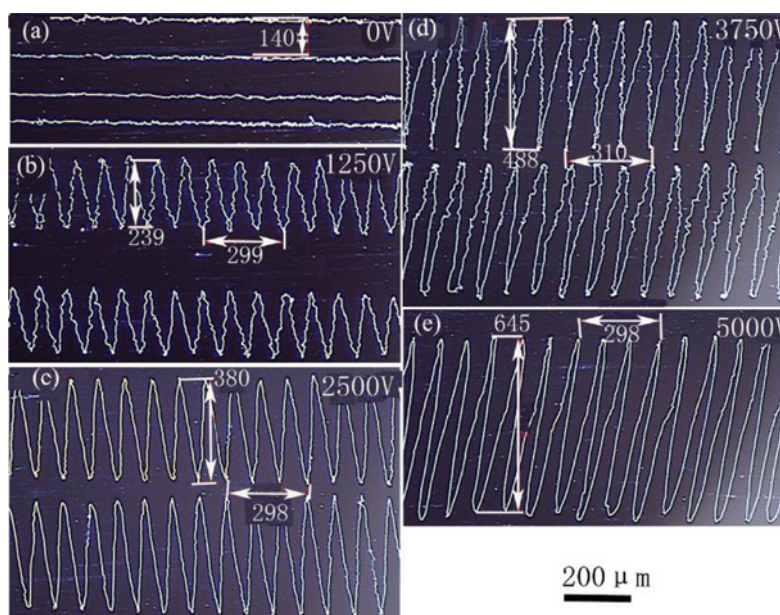


FIGURE 3.—CNC video measuring system picture; scale, 200  $\mu\text{m}$ . The experiment of ACP voltage parameter: (a) the ACP voltage is 0 kV, the deposited is a straight line, but the fiber is not smooth; (b) the ACP voltage is 1250 V, the amplitude of the fiber is 239  $\mu\text{m}$ , and the fibrous wavelength of three periods is the 299  $\mu\text{m}$ ; (c) the ACP voltage is 2500 V, the amplitude of the fiber is 380  $\mu\text{m}$ , and the fibrous wavelength of three periods is 298  $\mu\text{m}$ ; (d) the ACP voltage is 3750 V, the amplitude of the fiber is the 488  $\mu\text{m}$ , and the fibrous wavelength of three periods is 310  $\mu\text{m}$ ; (e) the ACP voltage is 5000 V, the amplitude of the fiber is 645  $\mu\text{m}$ , and the fibrous wavelength of the three periods is 298  $\mu\text{m}$ .



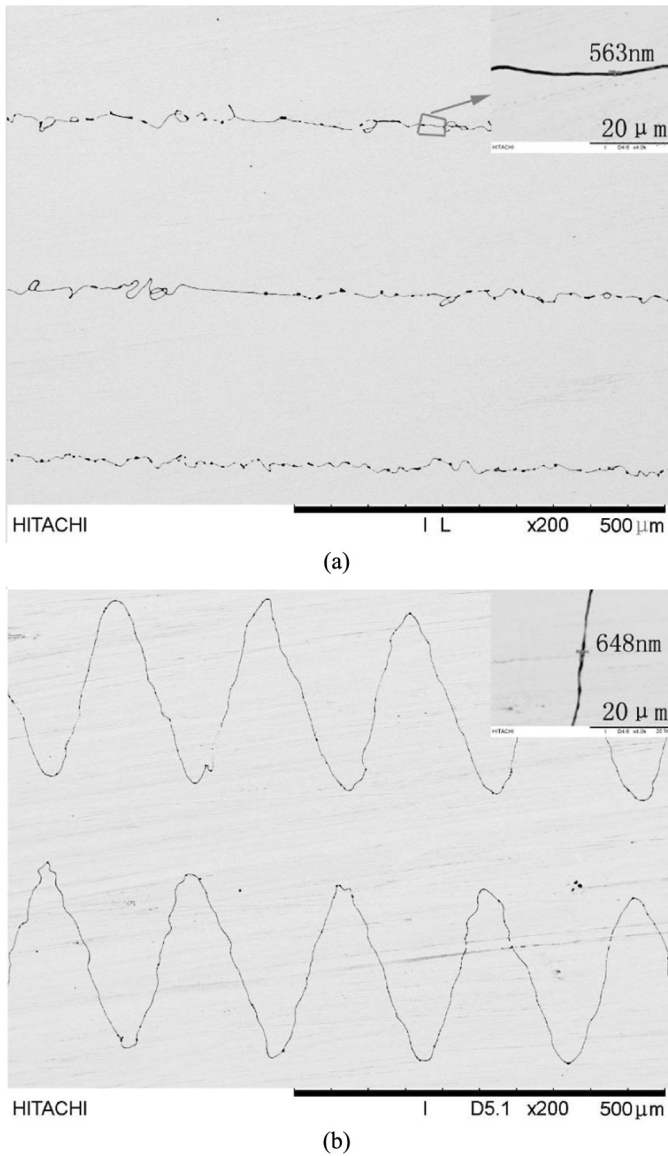


FIGURE 5.—SEM images of the fibers: the collector speed is 5 mm/s, the applied voltage to nozzle is 1 kV, the D-N-C is 4 mm, and the solution is 4 wt%. (a) shows that the ACP voltage is 0 V and the diameter is 563 nm; (b) the ACP voltage is 1250 V and the diameter of the fiber is 648 nm.

wavy/zigzag fibers can be controlled with the alternating electrical field force. However, the fibers would be rigid because the collector motion speed is less than the electrospinning rate during in NFES process as shown in Figs. 3(b) and 5(b). The falling jet in a relaxed state is easily disturbed by other factors, including the repulsive Coulomb force generated by the deposited fibers [15].

The ACP has a frequency that is an important factor affecting the morphology of the wavy fibers. The effect of the frequency of the ACP on wavy fibers deposition is also studied in this work. The experimental results are shown in Fig. 6(a)–(d) for each frequency parameter of ACP. When the jet is affected by the auxiliary electric

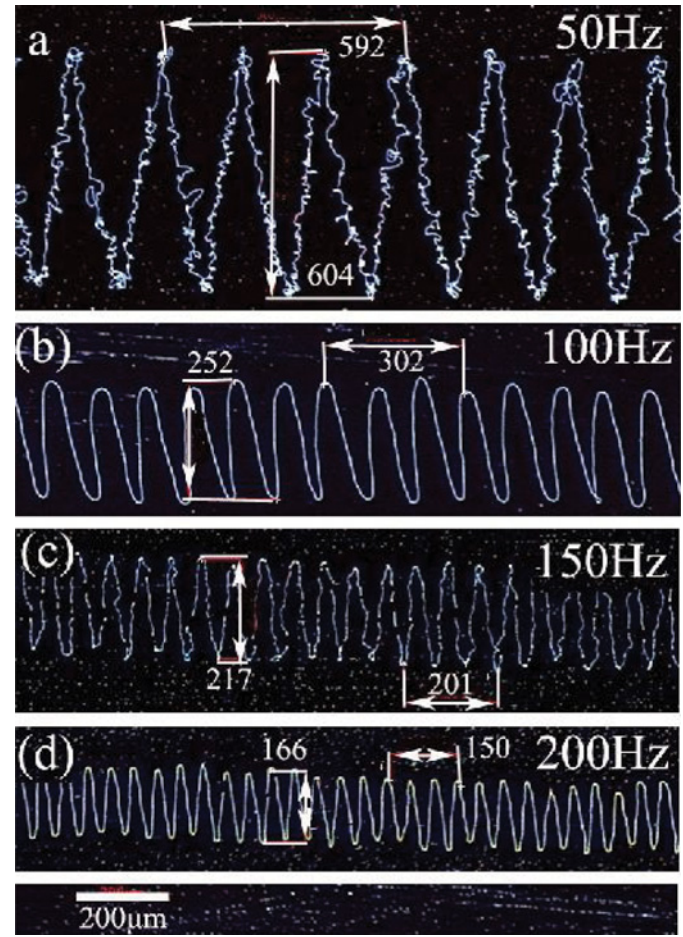


FIGURE 6.—CNC video measuring system picture; scale, 200 μm. (a) ACP voltage frequency of 50 Hz; fibrous amplitude of 604 μm; the fibrous wavelength of three periods is 592 μm. (b) ACP voltage frequency of 100 Hz; fibrous amplitude of 252 μm; the fibrous wavelength of three periods is 302 μm. (c) ACP voltage frequency of 150 Hz; fibrous amplitude of 217 μm; the fibrous wavelength of three periods is 201 μm. (d) ACP voltage frequency of 200 Hz; fibrous amplitude of 166 μm; the fibrous wavelength of three periods is 150 μm.

field, the jet would swing (Fig. 6(a)). Meanwhile, when the frequencies of ACP supply to the A-E increase, the jet swing process needs less time, and then the jet swinging distance is shortened, which results in the decreasing amplitude of the wavy fibers. Therefore, the amplitude of the wavy fiber decreases as the auxiliary electric field frequency increases. At the same time, it can be seen from Fig. 6(a)–(d) that when the frequency of the ACP increases, the wavelength in three periods decreases. The wavy fibers' generated frequency can be calculated by the following equations:

$$f = \frac{1}{T} \quad (1)$$

$$\lambda = v \times T \quad (2)$$

where  $f$  is the generated frequencies of wavy fibers;  $v$  is the collector speed;  $T$  is the generated period of the

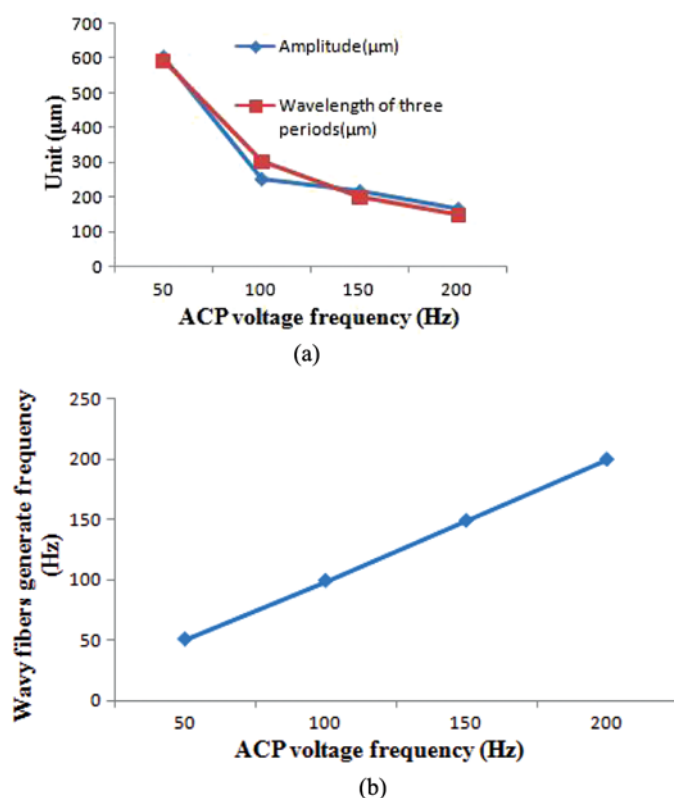


FIGURE 7.—(a) Fibrous amplitude and fibrous wavelength of three periods versus the ACP voltage frequency; (b) wavy fibers generated frequency versus ACP voltage frequency.

wavy fibers; and is the wavelength of the wavy fibers. The experimental results show that the fibrous amplitude decreases with the increasing ACP voltage frequency, and the wavelength of the wavy fibers in three periods also decreases with the ACP voltage frequency increase (Fig. 7(a)). It was also discovered that the generated frequency of wavy fibers is the same as the ACP frequency. Therefore, the wavelength of the wavy fibers can be controlled by the frequency of the auxiliary electric field and collector speed, which is valuable for micro-electromechanical system fabrication. Compared to other methods, Han et al. found that the patterns have frequencies of the order of  $10\text{--}10^6$  Hz, but were not able to precisely control the pattern frequencies [12, 13].

#### CONCLUSIONS

The wavy micro/nanofiber via A-E in NFES is studied in this paper. During electrospinning process, the charged jet is easily disturbed by many factors, including low collector speed. When the DC power voltage supplied to electrospinning is also low, the fiber deposited on the collector is not a straight line. When the ACP voltage is supplied to the A-E, the jet begins to swing, and the wavy fibers deposit on the motion collector. Meanwhile, the amplitude of the wavy fibers increases with the increasing ACP voltage. The frequency of the

wavy fibers is also studied in this paper, and the collector speed does not affect the wavy fibers' frequency. Additionally, the experimental results show that the wavy fibers frequency is the same as the ACP frequency.

#### FUNDING

This work was financially supported by National Natural Science Foundation of China (51305084), Guangdong Innovative Research Team Program (No. 201001G0104781202), Guangdong Provincial Key Laboratory of Micro-nano Manufacturing Technology and Equipment (GDMNML2013-1), Guangdong Provincial Key Laboratory Construction Project of China (Grant No. 2011A060901026), and Key Joint Project of National Natural Science Foundation of China (Grant No. U1134004).

#### REFERENCES

- Huang, Z.M.; Zhang, Y.Z.; Kotaki, M.; Ramakrishna, S. A review on polymer nanofibers by electrospinning and their applications in nanocomposites. *Composites Science and Technology* **2003**, 63 (15), 2223–2253.
- Sun, B.; Long, Y.; Zhang, H.; Li, M.; Duvail, J.; Jiang, X.; Yin, H. Advances in three-dimensional nanofibrous macrostructures via electrospinning. *Progress in Polymer Science* **2013**, 39 (5), 862–890.
- Manuelli, A.; Persano, L.; Pisignano, D. Flexible organic field-effect transistors based on electrospun conjugated polymer nanofibers with high bending stability. *Organic Electronics* **2014**, 15 (5), 1056–1061.
- Ren, Z.; Gao, P.-X. A review of helical nanostructures: Growth theories, synthesis strategies and properties. *Nanoscale* **2014**, 6 (16), 9366–9400.
- Kong, X.Y.; Wang, Z.L. Spontaneous polarization-induced nanohelices, nanosprings, and nanorings of piezoelectric nanobelts. *Nano Letters* **2003**, 3 (12), 1625–1631.
- Huang, Y.A.; Bu, N.B.; Duan, Y.Q.; Pan, Y.Q.; Liu, H.M.; Yin, Z.P.; Xiong, Y.L. Electrohydrodynamic direct-writing. *Nanoscale* **2013**, 5 (24), 12007–12017.
- Motojima, S.; Chen, Q.Q. Three-dimensional growth mechanism of cosmo-mimetic carbon microcoils obtained by chemical vapor deposition. *Journal of Applied Physics* **1999**, 85 (7), 3919–3921.
- Zhang, H.-F.; Wang, C.-M.; Buck, E.C.; Wang, L.-S. Synthesis, characterization, and manipulation of helical SiO<sub>2</sub> nanosprings. *Nano Letters* **2003**, 3 (5), 577–580.
- Reneker, D.H.; Yarin, A.L.; Fong, H.; Koombhongse, S. Bending instability of electrically charged liquid jets of polymer solutions in electrospinning. *Journal of Applied Physics* **2000**, 87 (9), 4531–4547.
- Yarin, A.L.; Koombhongse, S.; Reneker, D.H. Bending instability in electrospinning of nanofibers. *Journal of Applied Physics* **2001**, 89 (5), 3018–3026.
- Zhao, Y.Y.; Yang, Q.B.; Lu, X.F.; Wang, C.; Wei, Y. Study on correlation of morphology of electrospun products of polyacrylamide with ultrahigh molecular weight. *Journal of Polymer Science Part B—Polymer Physics* **2005**, 43 (16), 2190–2195.
- Han, T.; Reneker, D.H.; Yarin, A.L. Buckling of jets in electrospinning. *Polymer* **2007**, 48 (20), 6064–6076.

13. Han, T.; Reneker, D.H.; Yarin, A.L. Pendulum-like motion of straight electrified jets. *Polymer* **2008**, *49* (8), 2160–2169.
14. Sun, D.; Chang, C.; Li, S.; Lin, L. Near-field electrospinning. *Nano Letters* **2006**, *6* (4), 839–842.
15. Zheng, G.; Li, W.; Wang, X.; Wang, H.; Sun, D.; Lin, L. Experiment and simulation of coiled nanofiber deposition behavior from near-field electrospinning. In *2010 5th IEEE International Conference on Nano/Micro Engineered and Molecular Systems (NEMS)*; IEEE, 2010.
16. Xin, Y.; Reneker, D.H. Hierarchical polystyrene patterns produced by electrospinning. *Polymer* **2012**, *53* (19), 4254–4261.
17. Duan, Y.Q.; Huang, Y.A.; Yin, Z.P. Transfer printing and patterning of stretchable electrospun film. *Thin Solid Films* **2013**, *544*, 152–156.
18. Deitzel, J.M.; Kleinmeyer, J.D.; Hirvonen, J.K.; Tan, N.C.B. Controlled deposition of electrospun poly(ethylene oxide) fibers. *Polymer* **2001**, *42* (19), 8163–8170.
19. Li, D.; Ouyang, G.; McCann, J.T.; Xia, Y.N. Collecting electrospun nanofibers with patterned electrodes. *Nano Letters* **2005**, *5* (5), 913–916.
20. Sun, B.; Long, Y.Z.; Liu, S.L.; Huang, Y.Y.; Ma, J.; Zhang, H.D.; Shen, G.Z.; Xu, S. Fabrication of curled conducting polymer microfibrillar arrays via a novel electrospinning method for stretchable strain sensors. *Nanoscale* **2013**, *5* (15), 7041–7045.
21. Duan, Y.Q.; Huang, Y.A.; Yin, Z.P.; Bu, N.B.; Dong, W.T. Non-wrinkled, highly stretchable piezoelectric devices by electrohydrodynamic direct-writing. *Nanoscale* **2014**, *6* (6), 3289–3295.
22. Gu, B.K.; Shin, M.K.; Sohn, K.W.; Kim, S.I.; Kim, S.J.; Kim, S.-K.; Lee, H.; Park, J.S. Direct fabrication of twisted nanofibers by electrospinning. *Applied Physics Letters* **2007**, *90* (26), 263902.
23. Bellan, L.M.; Craighead, H.G. Control of an electrospinning jet using electric focusing and jet-steering fields. *Journal of Vacuum Science & Technology B* **2006**, *24* (6), 3179–3183.
24. Zheng, G.; Li, W.; Wang, X.; Wu, D.; Sun, D.; Lin, L. Precision deposition of a nanofibre by near-field electrospinning. *Journal of Physics D: Applied Physics* **2010**, *43* (41), 415501.
25. Liu, Z.H.; Pan, C.T.; Lin, L.W.; Huang, J.C.; Ou, Z.Y. Direct-write PVDF nonwoven fiber fabric energy harvesters via the hollow cylindrical near-field electrospinning process. *Smart Materials and Structures* **2014**, *23* (2), 025003.
26. Persano, L.; Camposeo, A.; Carro, P.D.; Fasano, V.; Moffa, M.; Manco, R.; D'Agostino, S.; Pisignano, D. Distributed feedback imprinted electrospun fiber lasers. *Advanced Materials* **2014**, *26* (38), 6542–6547.
27. Ru, C.H.; Chen, J.; Shao, Z.S.; Pang, M.; Luo, J. A novel mathematical model for controllable near-field electrospinning. *Aip Advances* **2014**, *4* (1), 017108.
28. Zheng, J.Y.; Liu, H.Y.; Wang, X.; Zhao, Y.; Huang, W.W.; Zheng, G.F.; Sun, D.H. Electrohydrodynamic direct-write orderly micro/nanofibrous structure on flexible insulating substrate. *Journal of Nanomaterials* **2014**, *2014* (2014), 7.
29. Bu, N.; Huang, Y.; Wang, X.; Yin, Z. Continuously tunable and oriented nanofiber direct-written by mechano-electrospinning. *Materials and Manufacturing Processes* **2012**, *27* (12), 1318–1323.
30. Grasl, C.; Arras, M.M.L.; Stoiber, M.; Bergmeister, H.; Schima, H. Electrodynamics control of the nanofiber alignment during electrospinning. *Applied Physics Letters* **2013**, *102* (5), 053111.
31. Arras, M.M.L.; Grasl, C.; Bergmeister, H.; Schima, H. Electrospinning of aligned fibers with adjustable orientation using auxiliary electrodes. *Science and Technology of Advanced Materials* **2012**, *13* (3), 035008.
32. Karatay, O.; Dogan, M.; Uyar, T.; Cokeliler, D.; Kocum, I.C. An alternative electrospinning approach with varying electric field for 2-D-aligned nanofibers. *IEEE Transactions on Nanotechnology* **2014**, *13* (1), 101–108.
33. Zheng, J.; Long, Y.Z.; Sun, B.; Zhang, H.D.; Zhang, J.C.; Huang, J.Y. Aligned nanofiber arrays and twisted nanofiber ropes via electrospinning with two frames collector. *Advanced Materials Research* **2013**, *690*, 523–526.
34. Wang, Y. Review of long period fiber gratings written by CO<sub>2</sub> laser. *Journal of Applied Physics* **2010**, *108* (8), 081101.
35. Di Camillo, D.; Fasano, V.; Ruggieri, F.; Santucci, S.; Lozzi, L.; Camposeo, A.; Pisignano, D. Near-field electrospinning of light-emitting conjugated polymer nanofibers. *Nanoscale* **2013**, *5* (23), 11637–11642.
36. Zhu, Ziming; Chen, Xindu; Zheng, Junwei; Liang, Feng; Li, Minghao; Wang, Han. Fabricate wavy micro/nano fiber via auxiliary electrodes. In *Proceeding of the 1st International Conference on Progress in Additive Manufacturing*, Nanyang Executive Centre, NTU, Singapore; Y.W.Y. Chua Chee Kai, Tan Ming Jen, Liu Erjia: Research Publishing: Singapore, 2014.
37. Wang, H.; Li, M.; Huang, S.; Zheng, J.; Chen, X.; Chen, X.; Zhu, Z. Deposition characteristics of the double nozzles near-field electrospinning. *Applied Physics A* **2014**, *118* (2), 621–628.
38. Han, W.; Minhao, L.; Xin, C.; Junwei, Z.; Xindu, C.; Ziming, Z. Study of deposition characteristics of multi-nozzle near-field electrospinning in electric field crossover interference conditions. *AIP Advances* **2015**, *5* (4), 041302.